IAU-ARAK

J. Iran. Chem. Res. 2 (2009) 121-131

Journal of the Iranian Chemical Research

www.iau-jicr.com

Numerical analysis of the optimal catalyst distribution in created unsteady state conditions

Yacine Benguerba *, Brahim Djellouli, Lemnouer Chibane, Lahcene Bencheikh

Laboratoire de Génie des Procédés Chimiques, Université Ferhat Abbas Sétif, 19000, Sétif, Algérie

Received 3 December 2008; received in revised form 24 May 2009; accepted 27 May 2009

Abstract

The determination of the optimal distribution of the catalytic activity profile, which maximizes the catalytic effectiveness, in created unsteady state conditions, is analyzed and treated numerically for the case of a simple reaction. It was proven that the modulation, of the temperature and the reactant concentration of the external bulk fluid, leads to a considerable increase of the catalytic effectiveness. The optimal active element distribution is a Dirac- δ function i.e. all the catalyst must be deposited at a specific distance from the center of the catalytic pellet. It was shown that this optimal position changes with time in a sinusoidal manner. This purpose can be achieved by the use of ultrasounds to artificially control the activity profile.

Keywords: Unsteady state; Optimal catalyst distribution; Forced perturbation; Temperature modulation; Concentration modulation

1. Introduction

The general objective of using nonuniform active phase distribution on an inert support in preparing chemical catalysts is to improve the performance of a catalyst pellet. In many works, treating this problem [2, 3, 6, 7, 8, 9, 10, 11, 12, 13], it is well established that the performances of the supported catalysts can be improved, in a significant way, by distributing the active element inside the inert support. This spatially nonuniform deposition of the catalytic active material leads to an improved catalytic performance–in terms of effectiveness, selectivity, resistance to deactivation, or in the prevention of the thermal runaway-. This is essentially due to the interactions between the chemical kinetics and the physical transport processes.

Morbidelli *et al*. [6, 7] prove analytically, for a Langmuir-Hinshelwood bimolecular reaction, that the optimal activity distribution is a Dirac-δ function, i.e., all the catalyst must be deposited in a specific position from the pellet center. Dougherty and Verykios [2, 3] employed a numerical search utilizing the orthogonal collocation method to integrate the state equations. They found, for the case of consecutive and parallel reactions, that the Dirac-δ function is the optimal activity distribution. Their study encompasses practically all the aspects of catalysis with nonuniformly activated catalysts. Vayenas and Pavlou [12], analyse the problem of the optimal active element distribution, in the presence or absence of the mass and heat transfer. They investigate the impact of different modes of transport on the optimal active element position and

* Corresponding author. Tel.: +98 4412780952; fax: +98 4412776707.
E-mail address: benguerbayacine@yahoo.fr (Y. Benguerba)

also on the catalytic performance. Baratti *et al*. [10, 11] show numerically that the catalyst distribution within the pellet is a Dirac-δ function. This result has been fully generalized by Wu *et al*. [9], for the most general case of an arbitrary number of reactions, following arbitrary kinetics and occurring in a nonisothermal pellet with finite external heat and mass transfer resistances.

The use of created unsteady state conditions by modulation of the temperature and the reactants concentrations is another way to improve the catalytic reactor yields. This technique shows increased transient reactions rates compared with those in the steady state conditions. Zhdanov [14] and Hansen [15] investigate theoretically and experimentally the effects of the modulation technique on the catalytic performance. They show that the kinetic rates increase with an improvement in the selectivity and a less catalyst deactivation.

Andreev *et al.* [16], study the impact of light field on the cooperative behaviour of adatoms on a homogeneous surface of dielectric, semiconductor, or metal. They demonstrate that lateral interaction of induced dipoles entails surface migration of adatoms in the radial direction beyond the illuminated area to form on it either a "crater" or, conversely, a "hump". Their result was applied by Andreev [17] in order to increase the productivity of porous catalyst granule. He proves that the effectiveness of various catalytic processes increases by creating artificially unsteady state conditions using ultrasounds. In this context, Andreev [18, 19] gives the conditions required to maximize the productivity of porous catalyst granules with a controlled activity profile and also the mathematical base for using ultrasounds in a homogeneous and a heterogeneous catalysis. Investigation of the critical phenomena on porous catalyst granule with a controlled activity profile was carried out to define the optimal operating conditions for such catalytic reactors [20].

The objective of this present work is to show the effects of modulation of the temperature and the reactants concentrations on the effectiveness by a numerical analysis, in the case of a simple reaction scheme, taking place in a nonisothermal symmetrical pellet, working under artificially created unsteady state conditions.

2. Formulation of the problem

Let us consider the simple chemical reaction

$$A \xrightarrow{k_1} Pr oduits \qquad (1)$$

For a nonisothermal reaction occurring in a symmetrical porous pellet with nonuniform active element distribution, the steady state mass and heat balance is given by [1]:

$$D_e \frac{1}{x^n}\frac{d}{dx}\left(x^n \frac{dC}{dx}\right) = a(x) r(C,T) \qquad (2a)$$

$$\lambda_e \frac{1}{x^n}\frac{d}{dx}\left(x^n \frac{dT}{dx}\right) = -(-\Delta H)\, a(x) r(C,T) \qquad (2b)$$

The rate constant density function *a(x)*, defined as the ratio of the local rate constant *k(x)* to its volume averaged value $\bar{k}$ [22, 23].

$$a(x) = \frac{k(x)}{\bar{k}} \qquad (3)$$

The density function must satisfy the following integral:

$$\frac{1}{V_p}\int_{V_p} a(x)\,dV = 1 \qquad (4)$$

The boundary conditions used here are given by:

$$\frac{dC}{dx} = \frac{dT}{dx} = 0\,;\ \ x = 0 \qquad (5a)$$

$$D_e\left(\frac{dC}{dx}\right) = k_c\left(C_f - C_R\right);\ \lambda_e\left(\frac{dT}{dx}\right) = h\left(T_f - T_R\right)\ ;\ \ x = R \qquad (5b)$$

Here it is supposed that the external concentrations and the temperature of the bulk fluid vary periodically with time, so that, the integral values in created unsteady state are equal to those in the steady state respectively.

$$C_f(t) = \tilde{C}_{f0} + \hat{C}_f(t)\,; \qquad \int_0^{\tau_1} \hat{C}_f(t)dt = 0 \qquad (6a)$$

$$T_f(t) = \tilde{T}_{fo} + \hat{T}_f(t); \qquad \int_0^{\tau_1} \hat{T}_f(t)dt = 0 \qquad (6b)$$

$$P_1\tau_1 = P_2\tau_2 = \tau \qquad (6c)$$

where $\tilde{C}_{f0}$ and $\tilde{T}_{f0}$ are the reactants concentrations and the temperature of the external bulk fluid in the steady state case conditions, respectively; P_1 and P_2 are arbitrary positive numbers; τ_1 and τ_2 are the periods of change of the functions $\hat{C}_f(t)$ and $\hat{T}_f(t)$.

For practical simplifications it is supposed that the periods of change τ_1 and τ_2 are significantly larger in comparison with the characteristic time of the catalytic process proceeding in the porous catalyst granule (quasi steady state) [17]. So, only the reactants concentrations (C_f) and the temperature (T_f) of the external bulk fluid (equation 5b) vary with time.

The functions of modulation (equations 6a and 6b) can be satisfied by using sinusoidal function:

$$C_f(t) = C_{f0} + C_{f0}\sigma_1\, sin(\omega t) \qquad (7a)$$

$$T_f(t) = T_{f0} + T_{f0}\sigma_2\, sin(\omega t) \qquad (7b)$$

where σ_1 and σ_2 are the amplitudes of the temperature and the concentration respectively, ω is the rotational frequency [s^{-1}]. We can introduce the dimensionless parameters:

$$u = \frac{C}{C_{f0}},\quad \theta = \frac{T}{T_{f0}},\quad s = \frac{x}{R},\quad B_{im} = \frac{k_c R}{D_e},\quad B_{ih} = \frac{hR}{\lambda_e},\quad \phi^2 = \frac{r(C_{f0},T_{f0})R^2}{D_e C_{f0}}$$

$$\beta = \frac{(-\Delta H)D_e C_{f0}}{\lambda_e T_{f0}},\qquad f(u,\theta) = \frac{r(C,T)}{r(C_{f0},T_{f0})},\quad \gamma = \frac{E}{R_G T_{f0}}$$

The equations (2a) and (2b) can be rewritten in the form:

$$\frac{1}{s^n}\frac{d}{ds}\left(s^n\frac{du}{ds}\right)=a(s)\phi^2 f(u,\theta) \quad (8a)$$

$$\frac{1}{s^n}\frac{d}{ds}\left(s^n\frac{d\theta}{ds}\right)=-\beta\phi^2 a(x) f(u,\theta) \quad (8b)$$

With the boundary conditions:

$$\frac{du}{ds}=\frac{d\theta}{ds}=0;\quad s=0 \quad (9a)$$

$$\frac{du}{ds}=B_{im}\left(1+\sigma_1 \sin(\omega t)-u_R\right);\ \frac{d\theta}{ds}=B_{ih}\left(1+\sigma_2 \sin(\omega t)-\theta_R\right);\ s=\mathbf{1} \quad (9b)$$

The dimensionless form of the equation (4) is given by:

$$(n+1)\int_0^1 a(s)s^n ds=\mathbf{1} \quad (10)$$

With the catalytic effectiveness defined by the following equation:

$$\eta(t)=(n+1)\int_0^1 f(u,\theta)a(s)s^n ds \quad (11)$$

The dimensionless kinetic term is given by:

$$f(u,\theta)=u.exp\left(\gamma\left(\mathbf{1}-\frac{\mathbf{1}}{\theta}\right)\right) \quad (12)$$

Since the effectiveness factor given by equation (11) is time-dependent, the time-average value is calculated and compared with that in the steady state conditions.

$$\overline{\eta}=\eta_{moy}=\frac{1}{\tau}\int_0^\tau \eta(t)dt \quad (13)$$

According to equation (13) there is an improvement of the effectiveness if the integral effectiveness $\overline{\eta}$ is greater than the effectiveness $\eta(0)$ in the steady state conditions.

3. Numerical procedure

The objective is to determine the value of the activity distribution *a(s)* which maximizes the performance index given by equation (11); and satisfies the constraint (10) and the diffusion-reaction equations (8a, 8b). The numerical resolution technique is based on the orthogonal collocation method [4, 5] with orthogonal polynomials given in (x^2) because of the concentrations and the temperature profiles symmetry. This method allows reducing a system of differential equations (8a, 8b) to a set of nonlinear algebraic equations. The number of internal collocation points *NC* was taken equal to 7.

$$\sum_{j=1}^{NC+1} B_{ij} u_j = a(s_i)\phi^2 f(u_i, \theta_i) \quad (14a)$$

$$\sum_{j=1}^{NC+1} B_{ij} \theta_j = -\beta . a(s_i)\phi^2 f(u_i, \theta_i) \quad (14b)$$

with $i = 1, NC$

Equations (9b) are used to calculate u_R (u_{NC+1}) and θ_R (θ_{NC+1}).

$$\sum_{j=1}^{NC+1} A_{NC+1,j} u_j = B_{im}\left(1 + \sigma_1 \sin(\omega t) - u_{NC+1}\right) \quad (15a)$$

$$\sum_{j=1}^{NC+1} A_{NC+1,j} \theta_j = B_{im}\left(1 + \sigma_2 \sin(\omega t) - \theta_{NC+1}\right) \quad (15b)$$

A and *B* are the first and second derivative matrices in the symmetrical orthogonal collocation method [4, 5] for different geometries (α=0: slab; α=1: cylindrical; α=2: sphere) and *NC* internal collocation points. In order to solve the system of the nonlinear algebraic equations (14a) and (14b) using the boundaries (15a) and (15b), the Newton-Raphson method is used. The values of the catalyst activity at the collocation points, unknown at this stage, were regarded as the adjustable parameters of the optimization problem. The objective function is given by equation (11), which can be evaluated by using the Gauss-Jacobi quadrature formulae, where the quadrature points coincide with the collocation points [5]. The search of the catalyst activity which maximizes equation (11) is operated with the ***Interior-point*** algorithm. This approach is used to solve a sequence of approximate constrained minimization problems.

In searching for the set of *a(i)* values, two constraints must be satisfied. The first one derives from the physical meaning of the activity function [10, 11]:

$$a(i) \geq 0 \qquad (i=1, N+1) \quad (14)$$

While the second is given by equation (10), which by using the Gauss-Jacobi quadrature formulae reduces as follows [10, 11]:

$$\sum_{i=1}^{N+1} a(i) w_i = 1/(\alpha + 1) \quad (15)$$

where w_i are the Lobatto weight functions [10, 11].

4. Results and discussion

4.1. The steady state regime

The effects of the heat of reaction β on the optimal activity distributions which maximize productivity or yield are shown in Fig. 1**.** It was found that the egg-white activity distribution is the optimal one. Increasing the value of the heat of reaction parameter leads to a significant intraparticle temperature gradients. So the catalytic activity shifts toward the pellet center to make best use of higher temperatures in this part of the catalyst.

Fig. 2 shows that for small values of ϕ (i.e. kinetic control) the inner activity distribution (egg-yolk) is the one which maximizes the effectiveness; for large values of ϕ (i.e. diffusion control) it was found that the outer activity distribution (egg-shell) is the optimal one; Finally,

for intermediate values of the Thiele modulus, the middle distribution (egg-white) has the highest effectiveness factor.

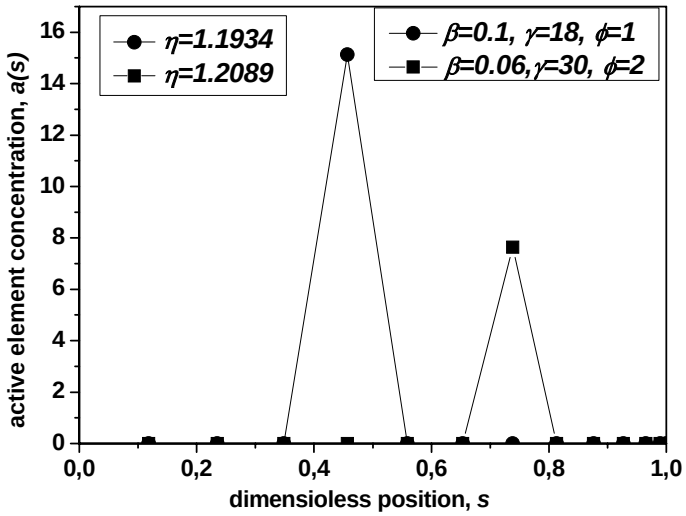

Fig. 1. The optimal catalyst distribution in steady state conditions.

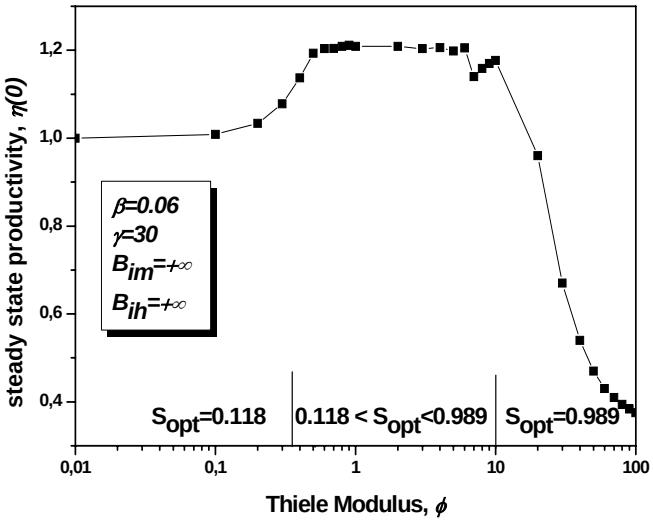

Fig. 2. The effects of the Thiele modulus on the productivity in unsteady state conditions.

4.2. The artificially created unsteady state regime

Fig. 3 shows the influence of the modulation of the concentration and the temperature on the effectiveness factor. The effectiveness factor varies with time in a sinusoidal manner having a peak in the neighbourhood of $t/\tau = 0.25$ which is the point where sinus function is equal to one. The modulation function is therefore maximal. The first half of the period is very characteristic of the enhancement process where the ratio $\eta(t)/\eta(0)$ (Enhancement factor) is greater than one. In the second half of period no enhancement was found (relaxation part). Fig. 4 shows that the time-average value $\overline{\eta}$ will be greater than the productivity in the steady state.

Fig. 5 shows that the optimal active sites location, $\overline{S}_{opt} = 0.73$ for the steady state case shifts, with increasing the modulation functions, to the outside of the pellet. This location allows the reduction of diffusion limitations. The location of optimal catalyst activity moves back to the interior of the pellet with decreasing the modulation functions.

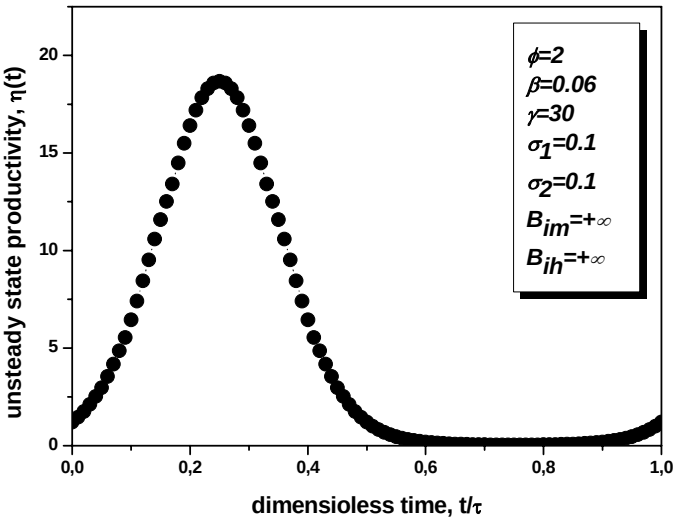

Fig. 3. The time variation of the catalytic productivity.

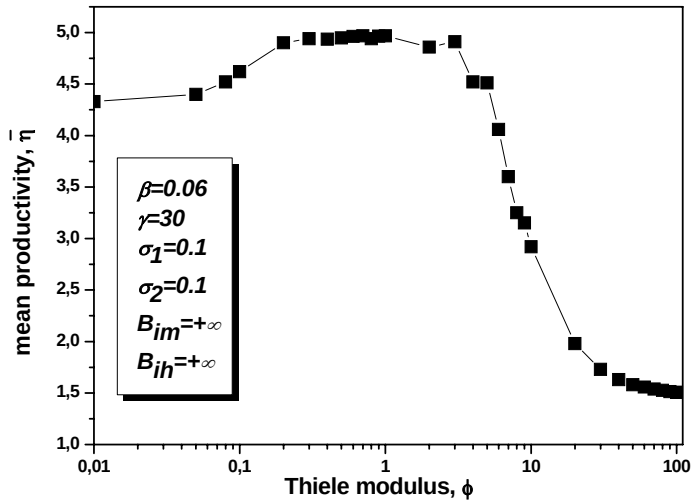

Fig. 4. The effects of the Thiele modulus on the mean productivity.

4.2.1. The effects of the Thiele modulus on productivity

Fig. 6 shows the variation of the effectiveness factor with the Thiele modulus. The ratio of the effectiveness in unsteady state conditions to the effectiveness in steady state was found to be always greater than one for practically all the values of the Thiele modulus.

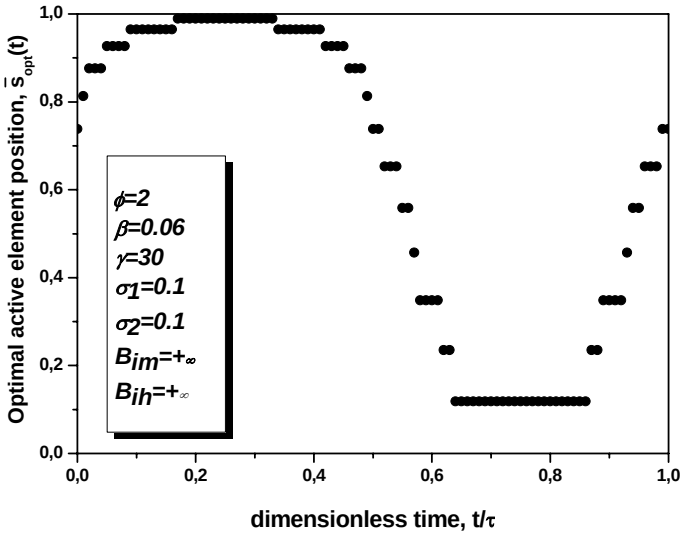

Fig. 5. Enhancement factor as a function of Thiele modulus.

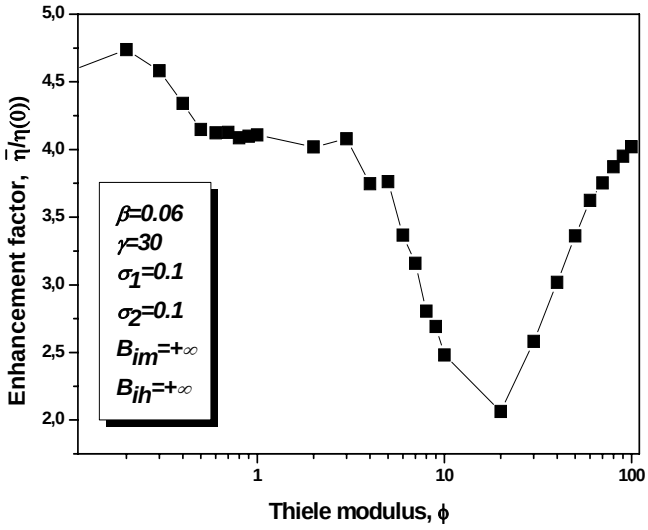

Fig. 6. The time variation of the location of the optimal catalyst distribution.

4.2.2. The effects of the Prater parameter β on the catalytic productivity

In this study the values of β was taken less than 0.15 to avoid problems of instability (Multiple steady states) according to Luss criterion [21] in the case of a nonisothermal first order simple reaction with external mass and heat transfer resistance. This Criterion, announces that stability domain is calculated by the following relation

$$\beta\gamma \leq \mathbf{4}\left(\frac{B_{im}}{B_{ih}} + \beta\right) \qquad (16)$$

Fig. 7 shows that increasing the value of β, increases the catalytic productivity for a moderate Thiele modulus. For high values of ϕ, less productivity was obtained.

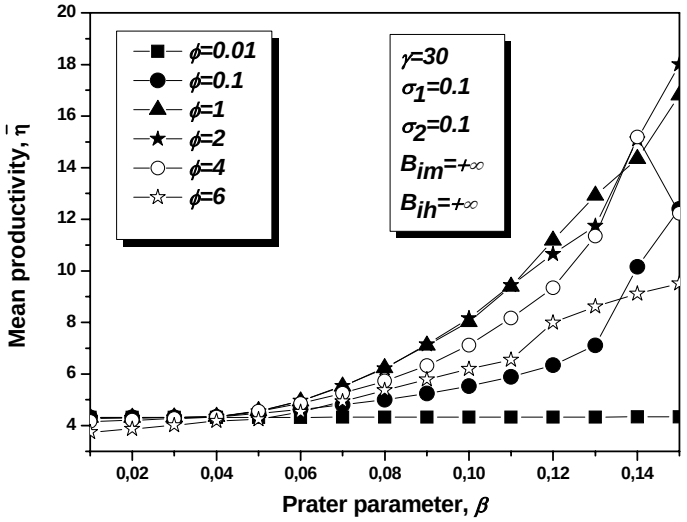

Fig. 7. The effect of the Prater parameter on the mean productivity.

Increasing the value of β, leads to an increase in the temperatures inside the catalytic pellet which can play a positive role in the catalytic act. The kinetic production inside the pellet becomes more important than at the surface of the pellet. The effectiveness factor is higher than one.

4.2.3. The effects of perturbation parameters

Fig. 8 shows the effects of the modulation of the concentration on the productivity. It is found that increasing σ_1 gives higher productivity than that obtained in the steady state conditions ($\sigma_1=0$). This increase is monotonous. Fig. 9 shows the effect of the modulation of the temperature on the productivity. As for the case of the modulation of the reactant concentration, the same result was found for the modulation of the temperature. The only difference is that the productivities calculated were hundred times higher than those calculated in the steady state conditions, for high σ_2.

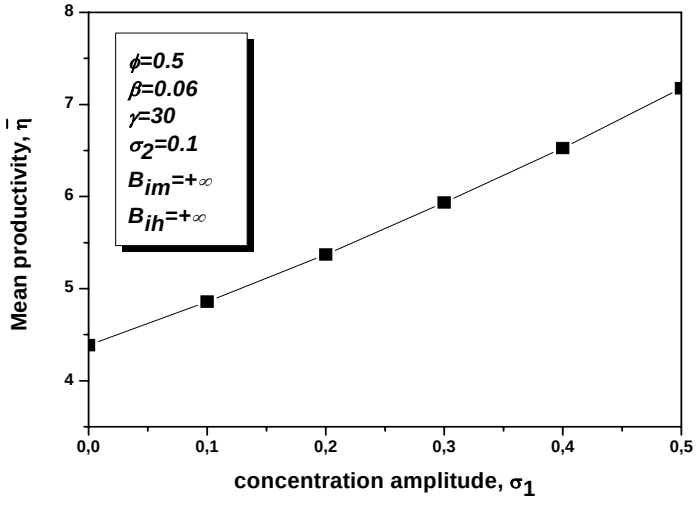

Fig. 8. The variation of the mean productivity with respect to amplitude σ_1.

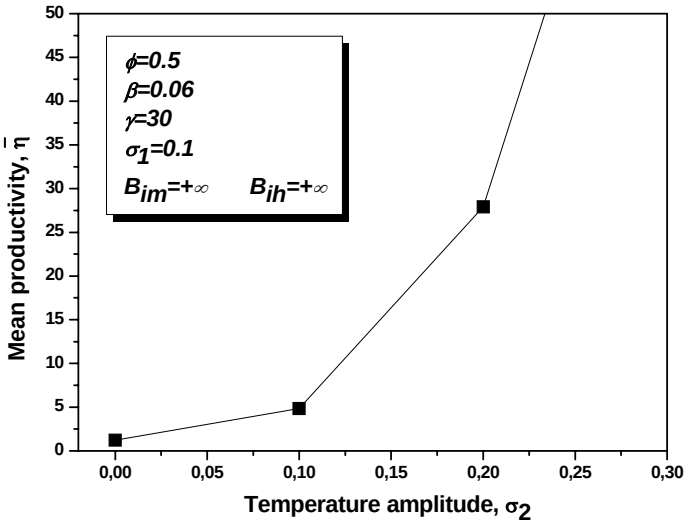

Fig. 9. The variation of the mean productivity with respect to amplitude σ_2.

5. Conclusion

The modulation, of the temperature and the concentrations of the external bulk fluid, investigated in this study, gives a good enhancement of the effectiveness factor which will increase the effective rate of the disappearance of reactants or the formation of products in the case of a simple reaction used in a fixed bed catalytic reaction. The numerical investigation has shown that the optimal catalyst distribution change in a sinusoidal manner. This purpose can be achieved by the use of an electromagnetic field like ultrasounds. It should be noted that the results of this study are theoretical and that the effects of some parameters on the productivity must be studied experimentally to confirm such results.

Notation

$a(s)$	Catalyst distribution function
B_{im}	Biot number of mass transfer ($k_c R / D_e$)
B_{ih}	Biot number of heat transfer (hR / λ_e)
C	Reactant concentration in solid phase, mol m^{-3}
C_f	Reactant concentration in fluid phase, mol m^{-3}
C_R	Reactant concentration at the surface of pellet, mol m^{-3}
D_e	Effective diffusion coefficient, m^2 s^{-1}
E	Activation Energy, cal mol^{-1}
$r(c,T)$	Rate of reaction, mol m^{-3} s^{-1}
$f(u,\theta)$	Dimensionless rate of reaction
h	Heat transfer coefficient, cal m^{-2} $K^{-1}s^{-1}$
k_c	Mass transfer coefficient, m s^{-1}
R	Radius of catalytic pellet, m
U	Dimensionless concentration
U_R	Dimensionless concentration at the surface pellet
R_G	Ideal gas constant, joule mol^{-1} K^{-1}
s	Dimensionless distance from center of the pellet
T	Temperature in solid phase, K
T_f	Temperature in fluid phase, K
T_R	Temperature at the surface of pellet, K

V_p Catalytic pellet volume, m^3
x Distance from the center of pellet, m

Greek Letters

w_i Lobatto coefficient
θ Dimensionless Temperature
ϕ^2 Thiele Modulus
β Dimensionless heat of reaction (Prater coefficient)
γ Dimensionless activation energy,$(E/R_G T_{f0})$
λ_e effective pellet thermal conductivity, cal K^{-1} m^{-1} s^{-1}
η_0 Catalyst effectiveness factor (productivity) in steady state regime
$\eta(t)$ Catalyst effectiveness factor (productivity) in unsteady state regime
$\overline{\eta}$ Mean effectiveness factor on period τ.

Acknowledgement

The authors would like to thank Professor V.V. Andreev from Chuvach state university (Russia) and Professor P. Légaré from Louis Pasteur university of Strasbourg (France) for their contribution in this present work.

References

[1] R. Aris, The Mathematical Theory of Diffusion and Reaction in Permeable Catalysts, Vol. 1. Clarendon Press, Oxford, 1975.
[2] R.C. Dougherty, X.E. Verykios, A.I.Ch.E. J. 32 (1986) 1858.
[3] R.C. Dougherty, X.E. Verykios, Catal. Rev. Sci. Eng. 29 (1987) 101.
[4] B.A. Finlayson, Nonlinear Analysis in Chemical Engineering, McGraw-Hill, New York, 1980.
[5] J. Villadsen, M.L. Michelsen, Solution of Differential Equation Models by Polynomial Approximation, Prentice-Hall, Englewood Cliffs, N.J. 1978.
[6] M. Morbidelli, A. Servida, A. Varma, Ind. Eng. Chem. Fund. 21 (1982) 278.
[7] M. Morbidelli, A. Varma, Ind. Eng. Chem. Fund. 21 (1982) 289.
[8] M. Morbidelli, A. Servida, S. Carra, A. Varma, Ind. Eng. Chem. Fund. 24 (1985) 116.
[9] H. Wu, A. Brunovska, M. Morbidelli, A. Varma, Chem. Eng. Sci. 45 (1990) 1855.
[10] R. Baratti, C. Giacomo, M. Morbidelli, Chem. Eng. Sci. 45 (1990) 1643.
[11] R. Baratti, H. Wu, M. Morbidelli, A. Varma, Chem. Eng. Sci. 48 (1993) 869.
[12] C.G. Vayenas, S. Pavlou, Chem. Eng. Sci. 42 (1987) 2633.
[13] R.M. Chemburkar, M. Morbidelli, A. Varma, Chem. Eng. Sci. 42 (1987) 2621.
[14] V.P. Zhdanov, Surface Science Reports, 55 (2004) 1.
[15] H.A. Hansen, J.L. Olsen, S. Jensen, O. Hansen, U.J. Quaade, Catalysis Communications 7 (2006) 272.
[16] V.V. Andreev, G.N. Ostryakov, G.G. Telegin, Chem. Phys. Reports 16 (1997) 159.
[17] V.V. Andreev, Mendeleev Communications 1 (1997) 35.
[18] V.V. Andreev, Mendeleev Communications 2 (1998) 43.
[19] V.V. Andreev, Ultrasonic Sonochemistry 6 (1999) 21.
[20] V.V. Andreev, A.V. Litvinenko, D.V. Lysenko, O.L. Figovsky, Sci. Israel-Tech. Adv. 2 (2000) 47.
[21] D. Luss, Chem. Eng. Sci. 26 (1971) 1713.
[22] W.E. Corbet, D. Luss, Chem. Eng. Sci. 29 (1974) 1473.
[23] J.B. Wang, A. Varma, Chem. Eng. Sci. 35 (1980) 613.